Sensorless Position Measurement Based on PWM Eddy Current Variation for Switched Reluctance Motor

Philippe Laurent, Bernard Multon, Emmanuel Hoang, Mohamed Gabsi

SENSORLESS POSITION MEASUREMENT BASED ON PWM EDDY CURRENT VARIATION FOR SWITCHED RELUCTANCE MACHINE

P. Laurent, B. Multon, E. Hoang, M. Gabsi
L.E.Si.R URA CNRS D1375
ENS Cachan, 61 Avenue du Pdt Wilson 94325 CACHAN CEDEX FRANCE
Tel: (33 1) 47 40 21 11 Fax: (33 1) 47 40 21 99

Abstract: This paper proposes a new method for indirect sensing of the rotor position in a switched reluctance motor. The method operates with the rotor eddy current losses produced by the PWM converter switching, regardless of magnetic saturation. Experimental results concerning sensitivity and performances are shown in a 6/4, 30w, 3000 rpm switched reluctance machine.

1. INTRODUCTION

In a Switched Reluctance Motor (SRM), the torque is developed by energizing phase winding in accordance with the rotor position. In order to avoid the use of a physical position sensor, a number of authors have proposed interesting solutions [1] [2]. These solutions can be easily divided into two main families:
The first group consists in measuring rotor position by mean of an unenergized phase.:
• Measuring the phase inductance by means of amplitude [3], [7] or frequency modulation [4] (problems of parameter sensitivity)
•Injecting a diagnostic pulse [5], [10] and measuring current ripple.
•Measuring the mutually-induced voltage [6] which requires significant interphase coupling.
•Flux estimation by means of a voltage integrator [8] and inductance calculation with simple phase model (the problem lies in model performance and integrator accuracy).
These methods are useful in both voltage and current controlled Switched Reluctance drives, but resolution decreases with the scanning window, especially at high speed. A second problem lies in the influence of the magnetic saturation when measuring the inductance profile.

A second group consists of high-level current or voltage sensing in an energized phase :
• Monitoring the current wave form [9]: difficulties are due to the internal back EMF influence and magnetic saturation.
• Measuring the current gradient in case of a voltage control (constant duty cycle) [2]. The method uses the influence of the back EMF on current wave form (a problem occurs at very low speed).
• More sophisticated methods are based on observations of the motor which determines the rotor position from voltage and current informations [11], [12]. This requires a powerful DSP for flux calculation. More over, magnetic coupling between phases is difficult to take into account.
Finally, other strategies do not require information about the rotor position, when it is assumed that the SRM always runs synchronously [13]. Only the dwell angle and frequency are adjusted in order to obtain robust control of speed.

2. CLASSICAL MODELIZING OF SRM

At the present time, sensorless control methods use the phase inductance measurement (by means of a scanning window or a flux calculation). So, there is a problem with the magnetic saturation that produces trouble-shooting with simple phase models. Thus, even with a powerful model, this problem causes a decrease in resolution measurement. We were looking for a new method using an electromagnetic parameter less sensitive to saturation. This could be obtained by use of the PWM eddy current losses which vary with the rotor position as well as the inductance phase. The PWM eddy current losses are independent of magnetic saturation. The problem in such a measurement concerns the influence of hysteretic losses which remain sensitive to saturation. We hope so that rotor PWM eddy current are preponderant.
The aim of the paper is to analysis the PWM eddy current losses which appear in the phase model as a classical resistor.(see Fig. 2)
In our case, we have a three-phase, 6/4, 30W 3000 rpm SRM fed by an asymmetrical half bridge converter (Fig. 1)

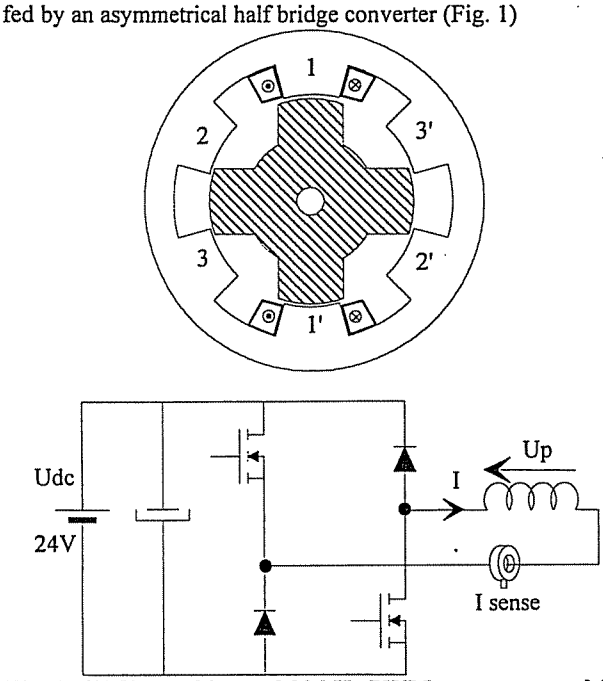

Fig. 1: 6/4 SR machine and 20 kHz PWM converter used for sensorless control.

For this kind of machine, we can adopt a classical single-phase transformer equivalent model for each stator phase such as proposed in Fig. 2. In this figure, Ro represents the ohmic coil resistor, Lf the leakage inductance, Rsi and Rri the yoke+ stator teeth and rotor equivalent eddy current loss resistor. In the case of a switched voltage supply control, the magnetic induction B does not depend on position in the yoke. B is also maximum for aligned position in rotor (hence the corresponding eddy current losses) and decreases when the rotor reaches the unaligned one. Rri is then a direct function of the electrical position θ.

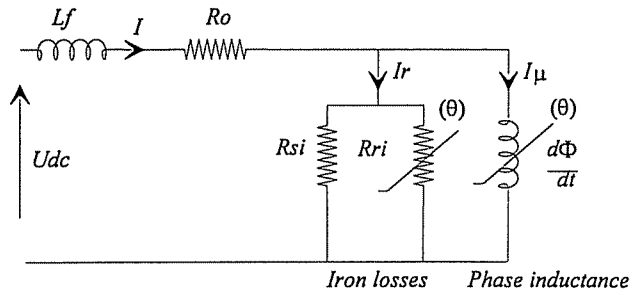

Fig 2.: simple phase model used for computer simulation

We obtain the following magnetizing equation:

$$U_{dc}=L_f.\frac{dI}{dt}+R_O.I+\frac{d\Phi}{dt} \quad (1) \text{ and } \quad \frac{d\Phi}{dt}=\frac{R_{si}.R_{ri}}{R_{si}+R_{ri}}.I_r \qquad (2)$$

In our case, for a 20kHz switching frequency, Lf and Ro are not significant in the simulation of the current ripple ($R_O.\Delta.I_r + Lf.\frac{dI}{dt} << \frac{d\Phi}{dt}$) and therefore a simpler equation can be obtained:

$$U_{dc} \approx \frac{d\Phi}{dt}+R_O.I \qquad (3)$$

where I is the DC value corresponding to magnetic state of the phase.

If we denote E, the internal EMF (due to speed and current) and Li the incremental inductance at a specified position:

$$U_{dc}=E+R_O.I+L_i.\frac{dI_\mu}{dt} \text{ and } U_{dc}=(\frac{R_{si}.R_{ri}}{R_{si}+R_{ri}}).I_r \qquad (4)$$

With our asymmetrical half bridge configuration (bipolar switching +Udc/-Udc), α represents the duty cycle and T the switching period: 50μs.

The final time variable equation for the magnetizing sequence is:

$$I_m(t)=\frac{U_{dc}}{L_i(\theta)}.(t)+\frac{U_{dc}}{R_{si}}+\frac{U_{dc}}{R_{ri}(\theta)}+I_{min} \qquad (5)$$

For the demagnetizing sequence the equation is similar:

$$I_d(t)=-\frac{U_{dc}}{L_i(\theta)}.(t-\alpha.T)-\frac{U_{dc}}{R_{si}}-\frac{U_{dc}}{R_{ri}(\theta)}+I_{max} \qquad (6)$$

Near the switching instant, ($t=\alpha.T$ for example), we can calculate Im-Id. In that case, a interesting result is obtained:

$$\Delta_{I_r}=I_m(\alpha.T)-I_d(\alpha.T)=2.\left(\frac{U_{dc}}{R_{si}}+\frac{U_{dc}}{R_{ri}(\theta)}\right) \qquad (7)$$

We can observe a discontinuity in the current waveform dependent on the rotor PWM iron losses variation. This is shown in Fig. 3 which corresponds to an experimental result. The square wave signal represents the stator phase voltage delivered by power converter, and we can easily note the current ripple discontinuity described in equation (7) at each switching instant.

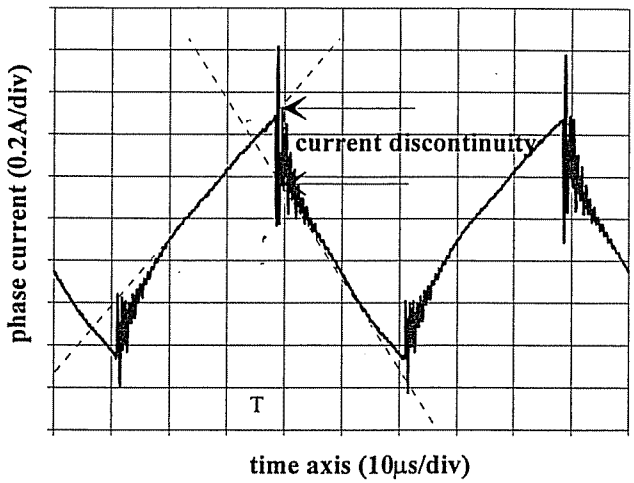

Fig. 3: experimental observation of current wave form with an asymmetrical half-bridge converter (24V, 20kHz).

3. INDIRECT ROTOR POSITION SENSING PRINCIPLE

The problem in controlling SRM is to determine the exact instant of the phase switching instant from a winding to another.

As we impose the stator flux level in the phase by means of a voltage PWM control, only the rotor induction level is dependent on the rotor position. We have seen that Rri (rotor iron losses parameter) was varying in accordance with rotor position. We can subsequently observe that the current ripple discontinuity represents an image of the rotor iron losses.

A first method consists in sampling current value at two separate instants ($\frac{\alpha.T}{2}$ and $\frac{T+\alpha.T}{2}$)which allow to obtain the desired current ripple discontinuity (Id-Im). Then we can determine an image of the position by reference to a look-up table. Different problems occur: discontinued current feeding mode, influence of the ohmic resistor and above all accuracy of sampling instant.

A more precise method was obtained by using the PWM voltage such as an high frequency scanning carrier of the phase magnetic model. The synopsis of the method is presented in fig. 4. The microcontroller generates the PWM duty cycle corresponding to a specified torque reference. We use the same clock signal to feed a selective band-pass switch capacitor filter and we obtain the fundamental value of the square wave voltage applied to the stator phase. It is also possible to connect the voltage filter to a sensing coil magnetically coupled with the main phase coil in order to eliminate the ohmic resistor influence .

The same kind of filter operates with the phase current and gives information about the fundamental of PWM current ripple. Finally, two sinusoidal signals describing the inductive and resistive parameter of the magnetic model are obtained.

Thanks to a synchronous demodulation ($\frac{\pi}{2}$ after zero crossing of voltage signal) we obtain the desired active component of magnetic current which corresponds to the desired resistive parameter.

Concerning the torque/current control of the machine, we decided to use a non linear regulator. This allows us to fix easily a minimum and maximum value of the duty cycle which is necessary for the sensorless measurement system.

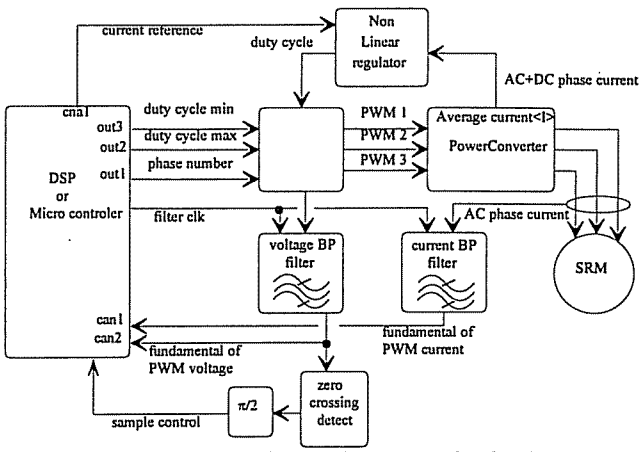

Fig. 4: block diagram of sensorless control using PWM as scanning carrier for determination of PWM eddy current losses.

The use of switch capacitor filter gives us an high accuracy concerning phase difference measurement between voltage and current waveforms. These filters are synchronised with the PWM control in order to eliminate switching noise and sliding phenomena in the final output waveform (more precise sample value is finally obtained).
This method also permits to measure the inductive parameter of phase model if the sample instant corresponds to the zero voltage crossing.

4. INFLUENCE OF MAGNETIC SATURATION

In order to study the influence of magnetic saturation upon the resistive parameter of the phase model, we have fed the phase machine by a 20kHz PWM voltage in addition to a DC bias current. We can compare the resistive and inductive parameter variation for different rotor positions (Fig. 5 and Fig. 6). In Fig. 5, we present the evolution of the inductive parameter versus rotor position and DC bias current. We can see in this figure that the incremental inductance of the phase remains very sensitive to the magnetic saturation especially when the rotor reaches the aligned position.

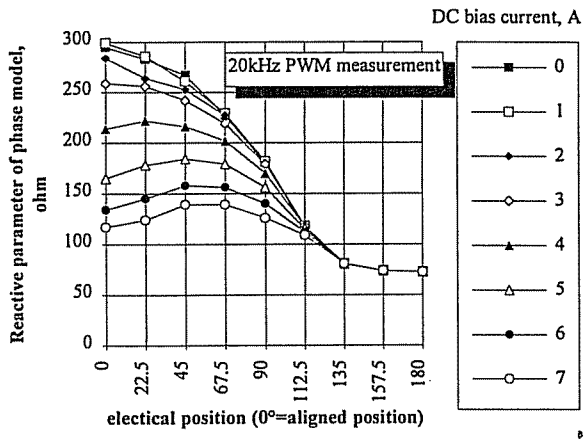

Fig. 5: evolution of reactive phase parameter Li versus rotor position for several DC bias current levels.

In that case, a sensorless control could not work properly in accordance with this parameter. In fig . 6, we present the evolution of the iron losses equivalent parameter versus rotor position and DC bias current. We can note that this parameter is also dependent on the magnetic saturation at aligned position. In that position, iron losses remain mainly dependent of magnetic saturation. This can be observed from the unaligned up to the exact middle position between aligned and unaligned position. This property was confirmed with finite element simulation and will be used in the experimental synopsis. We also observe that in very low magnetic bias condition, the total iron losses decrease at aligned position.

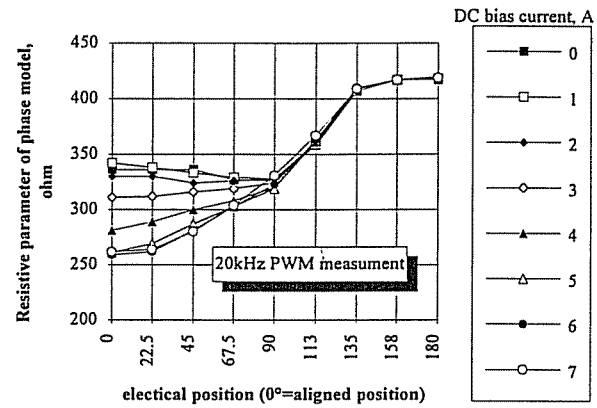

Fig. 6: evolution of iron losses equivalent parameter Rsi and Rri versus rotor position for several DC bias current levels.

Concerning inductive parameter, the classical magnetic saturation causes the decrease of the incremental inductance. It's because most of sensorless method using this parameter variation need to take this non linear phenomenon into account in order to work properly.
For the resistive one, an explanation lies in PWM hystereric current that is sensitive to the magnetic permeability such we have already observe in a previous paper [7].
This leads to think that there is no magnetic saturation insensitive parameter in an SRM but the eddy current losses parameter allow a quite good measurement of the position from the unaligned one up to the middle one between aligned and unaligned. . A solution is to measure an intermediate position on which magnetic saturation has low influence. Its the aim of the following software algorithm.

5. SPEED INFLUENCE

The speed influence effects are considerably reduced because of the use of very selective filters in the determination of the phase model parameter. In the magnetizing equation the back emf spectrum does not occur in the final demodulated voltage and current waveform thanks to the high frequency PWM used in example (20kHz). We can eliminate this problem by using a separate AC current sensor constituted with a standard magnetic tore measuring simultaneously the three phases current. The advantage of this method lies in the fact that this kind of measurement provides a natural built-in high-pass filter and the global magnetic level in the tore remains unchanged when the supply is switched from one phase to the following one. Thanks to this method there is no floating voltage induced during this phase commutation and only one sensor is needed.

Concerning resolution of the method, if Ω denotes the mechanical rotor speed (rpm) and Nr the number of rotor poles (Nr=4 in our example) the electrical frequency is Fe:

$$F_e = \frac{\Omega . N_r}{60} \text{ (example Fe=200Hz at 3000 rpm)} \quad (9)$$

In the case of q phase machine, the duration of each scanning window Tscan corresponds to the maximum supply window:

$$T_{scan} = \frac{1}{q . F_e} \text{ (ex:1.66ms for a 3 phases and 3000 rpm)} \quad (10)$$

Then each period of the PWM provides one point of position measurement so the global resolution Np (the number of points per supply depends on the choice of the PWM frequency and decreases linearly at high speed:

$$N_p = F_{pwm} . T_{scan} = \frac{F_{pwm} . 60}{q . \Omega . N_r} \quad (11)$$

For example (10) provides a resolution of 33 points per electrical period of measurement at 3000rpm and 20kHz PWM frequency which is enough to ensure a good positioning of the supply window.

6. PWM CURRENT REGULATOR.

We can see in fig. 4 a non linear current regulator. This type of regulator works by regulating the maximum value of the DC current according to the current reference (current reference is given by the torque reference).
When the desired current value is reached, the system holds the power converter off until the end of the switching period and then releases it for the following sequence. The problem is to ensure that there will be at least one commutation during the switching sequence and then we fix a minimum and maximum value of the duty cycle. The regulator will then work naturally between these two limits in order to tune the phase current in accordance with the reference.
Another solution consists in using a classical numerical PI regulator but it requires a quite powerful DSP to ensure a complete calculation during the switching period. These two methods have been tested and better results are obtained whith a non linear regulator which is simpler.

7. EXPERIMENTAL RESULTS

We present in Fig. 7 an example of a phase current waveform whith a constant PWM duty cycle (ch2) and the corresponding fundamental harmonic finally obtained after a band-pass filtering operation (ch1).
We can easily note that the system works properly and gives good accuracy by using a very low current ripple (because of the 20kHz PWM and low voltage application). The maximum value of the sinusoidal waveform corresponds to the beginning of the supply window (the unaligned position in motor mode) and decreases as the rotor reaches the aligned one (maximum value of phase inductance).
It is interesting to notice that the back emf modifies the global phase current wave-form but has non influence upon the final filtered wave form. This confirms our assumption concerning the low influence of speed(c.f. *f* 5).

A classical sensorless control working directly with the envelop of this sinusoidal wave-form has been tested and gives very good results even during speed transitional conditions.

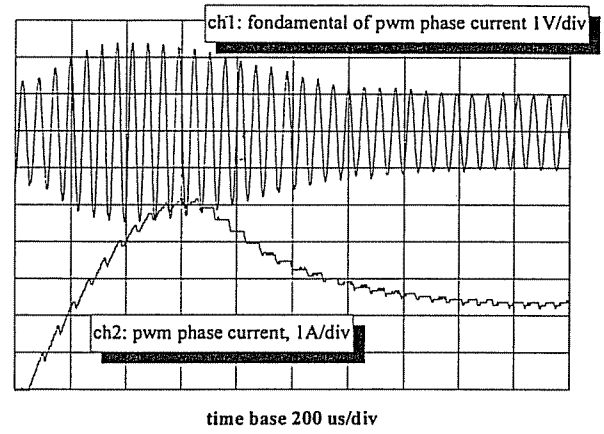

Fig. 7: oscillogram of the DC phase current (ch2) and the corresponding fundamental harmonic obtained after band pass filtering, 2000 rpm.

After each phase switching the system needs only a few PWM periods to stabilize at the correct value of the fundamental harmonic current and allows a measurement of the position.
The same filtering method works with the supply voltage applied to the energized phase and provides a sinusoidal voltage amplitude varying with the duty-cycle instantaneous value. By using two limits for the duty cycle range it is possible to limit the variation of the corresponding fundamental harmonic value.
We have studied the influence of the duty cycle value upon the measurement method accuracy. Results are presented in fig. 8 in the case of bipolar $+U_{dc} / -U_{dc}$ PWM mode.
If h denotes the harmonic number, the classical AC square-wave voltage (+E/-E) harmonic amplitude (a_h)with variable duty cycle α is expressed as follow:

$$a_h = \frac{2.E.(1-\alpha)}{\pi.h} . [sin(\alpha.\pi.h)] - \frac{2.E.\alpha}{\pi.h} . [sin(\pi.h) - sin(\alpha.\pi.h)] \quad (12).$$

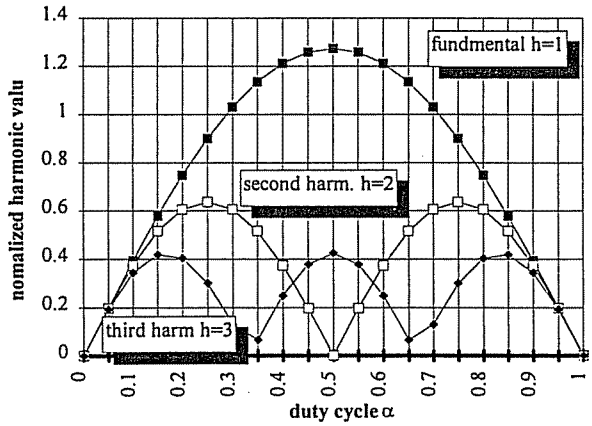

Fig. 8: calculation of PWM voltage harmonic versus PWM duty cycle α

We note that the scanning carrier amplitude, corresponding to the PWM fundamental voltage decreases as soon as the duty cycle α reaches 1 or 0. It is because we have decided to choose two duty cycle edges in order to ensure a quite good

measurement of the AC current component. For example if we limit α from 0.2 towards 0.8 the fundamental harmonic (h=1) only varies ±20% around 1. It is interesting to notice that in most case of duty cycle ($\alpha \approx 0.5$) the second and third harmonic do not perturb the fundamental harmonic filtering. This allows us to reduce the filtering order and then a simple fourth order band pass filter with a resonance factor equal to 3 gives very good results for a wide range of duty cycle value (see fig. 8).
In fig. 9 we present the final synchronous demodulated current corresponding to the PWM eddy current losses.

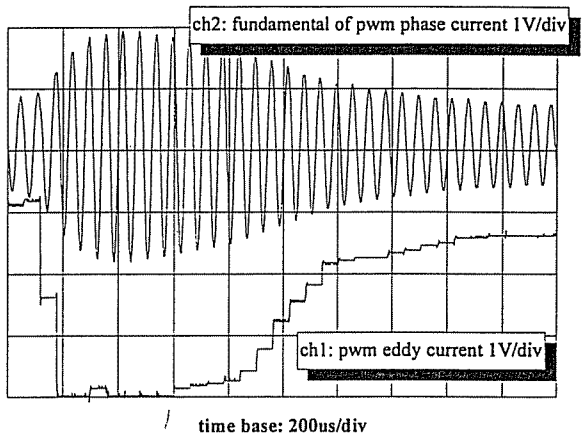

Fig. 9: example of harmonic current (ch2) and its corresponding PWM eddy current demodulated waveform obtained with synchronous sampling (ch1); 2000 rpm.

The sample order is provided by a zero crossing detector and controls the voltage and current analog to digital conversion. A fine tuning of this sample instant is necessary if we need to obtain the exact active component of the total PWM current waveform. The Maximum value of PWM eddy current is obtained for the aligned rotor position which generally corresponds to the end of the supply window. The Maximum resolution in the demodulated signal is obtained approximately for the intermediate position between aligned and unaligned position. This area is also fairly insensitive to the magnetic saturation (see Fig. 6). This is the reason because we have decided to use a specific algorithm in order to synchronize a numerical counter with this particular position.
The idea is to reset an internal count each time this position is detected and then order the phase switching at the middle count. We present the corresponding algorithm in fig. 10.
The global computed program is built around an interrupt process which is activated at each switching instant. The DSP used for this experimentation is a 56001 Motorola chip but a cheaper microcontroller is suitable.

After a simple step-by-step start-up of the SRM the process is able to synchronize almost immediately to the correct duration value of the supply window. An internal temporisation avoids noise influence after reference position detection (section edge detector) and holds the last measurement until tempo is terminated (trigger equivalent system).
When the tempo is terminated the system waits until the next reference position is reached and initiates its internal position counter. The reference phase switching default instant corresponds to the middle count of this integrator and it is then possible to tune very precisely the dwell angle by adjusting this switching position.

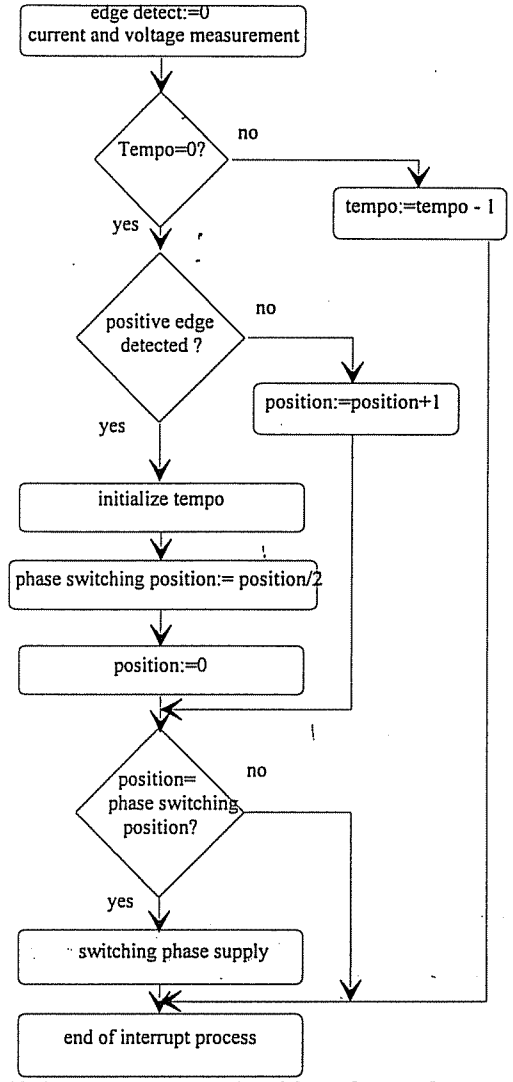

Fig. 10: interrupt process algorithm of sensorless control.

This allows us to improve the SRM torque characteristic especially at high speed condition with quite good accuracy.
This algorithm was tested and gives quite sufficient results especially during the transient between open loop and closed loop control.
We present in fig 11 an example of this demodulated PWM eddy current waveform and the corresponding internal position integrator at steady state running .

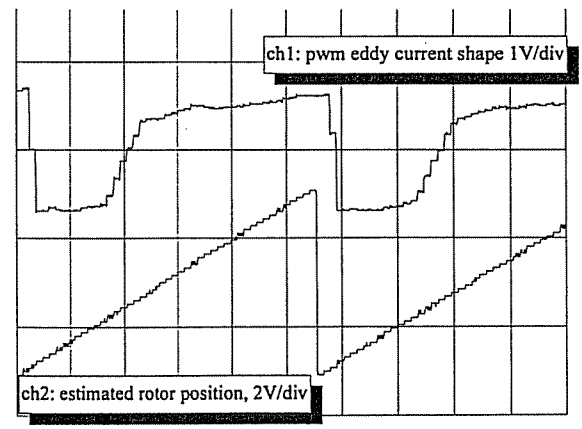

Fig. 11: example of PWM eddy current waveform and corresponding position estimation at steady state running.

By measuring the intermediate position of the supply window corresponding to the counter resetting it is very easy to shift the supply window and so improve the high speed performances of the motor. In that case the corresponding phase switching instant will no longer correspond to the exact half value of the counter but to a closeness one easily computed before.

8. CONCLUSION

A new technique has been proposed and investigated for the sensorless operation using PWM iron losses variation versus rotor position. Successful experiments can be obtained in addition with specific algorithm which allows us to reduce magnetic saturation influence. It appears clearly that the approach gives many inherent advantages:

- the scanning carrier is directly provided by the PWM power supply.
- the position resolution increases with the PWM frequency
- it is essentially independent of the motor speed and allow high transient speed variation.
- it possesses an intrinsically high noise immunity due to the synchronous band-pass filter and demodulation method.
- it allows to adjust the dwell angle very precisely according to an angle look-up table. High speed performance can be finally obtained.

Unfortunately, even PWM iron losses are slightly dependent on magnetic saturation and we do not think that another phase parameter could eliminate this problem. One solution was proposed using a specific software which determines one rotor position that is not affected by saturation.
However, the method has been integrated into a microcontroller and closed loop sensorless control for a three phase variable reluctance machine has been achieved. Wide range of speed is possible (3000rpm) and the upper limit is only dependent of the pwm frequency. The system is able to start-up after half round open loop step by step operation.

9. REFERENCES

[1] W.F. RAY L.H. AZI-BAHADLY
"Sensorless Methods for Determining the Rotor Position of Switched Reluctance Motors."
Proceedings of EPE 93, Vol 6, 1993, pp 7-13

[2] P. CARNE KJAER
"A New Indirect Rotor Position Detection Method for Switched Reluctance Motors."
Proceedings of ICEM 94, Vol 2, 1994, pp 555-560

[3] M. EHSANI, I.HUSAIN, A.B. KULKARNI
"Elimination of Position and Current sensor in Switched Reluctance Motor Drives."
IEEE Trans I.A., Vol 28, n°1, 1992, pp 128-135

[4] M. EHSANI, S. MAHAJAN, K.R. RAMANI, I.HUSAIN
"New Modulation Encoding Techniques for Indirect Rotor Position Sensing in Switched Reluctance Motors."
Proceedings of IEEE IAS 92, Vol 1, 1992, pp 430-438

[5] N.H. MVUNGI, J.M. STEPHENSON
"Accurate Sensorless Rotor Position Detection in a S. R. Motor."
Proceedings of EPE 91, Vol 1, 1991, pp 390-393

[6] M. EHSANI, I HUSAIN
"Rotor Position Sensing in Switched Reluctance Motor Drives by measuring Mutually Induced Voltage."
Proceedings of IEEE IAS Houston 92, Vol 1, 1992 pp 422-429

[7] P. LAURENT, M. GABSI, B. MULTON
"Sensorless Position Analysis using Resonant Method for Switched Reluctance Motors."
Proceedings of IEEE IAS Toronto 93, Vol 1 1993, pp 687-694

[8] M. EGAN, M.B. HARRINGTON, J.M.D. MURPHY
"PWM based Position Sensorless Control of Variable Reluctance Motor Drives."
Proceddings of EPE 91, Vol 4, 1991, pp 24-29

[9] P. ACARNELEY, R. HILL, C. HOOPER
"Detection of Rotor Position in Stepping And Switched Reluctance Motors by Monitoring of Current Waveforms".
IEEE Trans. I.A. Vol 28, n°6, Nov/Dec 1992, pp 133-142.

[10] S.R. MACMINN, W.J. RZESOS, P.M. SZCZESNY, T.M. JAHNS
"Application of Sensor Intégration Techniques in Switched Reluctance Motor Drives".
IEEE Trans. I.E. Vol 28, n°6, Nov/Dec 1992, pp 1339-1343.

[11] J.H. LANG, A. LUMSDAINE
"State Observers for Variable Reluctance Motor".
IEEE Trans. on I.E., Vol 37, n°2, 1990, pp 133-142.

[12] C. ELMAS, H. ZELAYA de la PARRA
"Position Sensorless Operation of a Switched Reluctance Drive Based on a State Observer".
Proceedings of EPE 93 Brighton , Vol 6, 1993, pp 82-87.

[13] T.J.E. MILLER, J.T. BARS, M. EHSANI
"Robuts Torque Control of Switched Reluctance Motors Without Shaft Sensor".
IEEE Trans on I.E., Vol IE33, n°3, 1986, pp 212-216.

10. ADRESS OF AUTHORS

P. LAURENT, B. MULTON, E. HOANG, M. GABSI
Laboratoire d'Electricité SIgnaux et Robotique URA D1375
61 venue du Pdt WILSON
94235 CACHAN CEDEX
FRANCE
☎ (33) (1)47 40 21 11
FAX (33) (1) 47 40 21 99
Mail: LAURENT@ens-cachan.fr